Chalcogenide Letters Vol. 22, No. 1, January 2025, p. 77 - 89

The effect of aluminum doping on nanostructured CdS: optical, structural and sensing characterization

H. R. Shakir [a], O. A. Chichan [b], M. S. Sada [c,*], S. A. Hussein [d], S. S. Chiad [e], N. F . Habubi [f], Y. H. Kadhim [g], M. Jadan [h,i]

[a] *Department of Optometry, Technical Medical Institute - Al-Mansur, Middle Technical University, Iraq.*

[b] *Department of Physics, College of Education for Pure Sciences, University of Babylon, Iraq.*

[c] *Department of Physics, College of Education, University of Masan, Iraq.*

[d] *Department of Medical Laboratory Techniques, Al-Manara College for Medical Science, Iraq*

[e] *Department of Physics, College of Education, Mustansiriyah University, Iraq.*

[f] *Department of Radiation and Sonar Technologies, Alnukhba University College, Iraq*

[g] *Department of Optics Techniques, College of Health and Medical Techniques, AL-Mustaqbal University, Babylon, Hillah, 51001, Iraq*

[h] *Department of Physics, College of Science, Imam Abdulrahman Bin Faisal University, P.O. Box 1982, 31441 Dammam, Saudi Arabia*

[i] *Basic and Applied Scientific Research Center, Imam Abdulrahman Bin Faisal University, P.O. Box 1982, 31441 Dammam, Saudi Arabia.*

CdS, and CdS: Al were grown onto glass bases via Chemical spray pyrolysis (CSP). XRD analysis of CdS films indicates a polycrystalline hexagonal structure with a predominant orientation of the (101) plane. The strain decreased from 28.55 to 25.66, and the grain size of undoped CdS films was around (13.51–12.14) nm as Al content rose. According to the results of AFM, CdS, CdS:2% Al, and CdS:4% Al all exhibit smooth surfaces with decreasing particle size in the range of (78.46), (69.75), and (42.20) nm, respectively. The root-mean-square roughness values for CdS and CdS:4% Al were 12.41 nm and 3.38 nm. According to AFM image, the surface roughness of CdS to CdS:4% Al were (9.74-5.16) nm. SEM images depict CdS films transitioning from flat islands (Undoped CdS) to uniform spherical nano-grains with Al doping. The result shows a decrease in absorption coefficient as Al content increased. The optical bandgap increased from (2.35-2.51) eV after doping. Results show that the extinction coefficient and refractive index are influenced by Al content. CdS film detects NO_2 gas by resistance increase, impacted by Aluminum doping. Sensitivity decreases with an increase in Al doping in CdS films.

(Received November 8, 2024; Accepted January 17, 2025)

Keywords: CSP, CdS: Al, XRD, Morphology and Optical properties

1. Introduction

II-VI semiconductors are receiving more attention, especially from the solar and optoelectronic sectors. With their broad direct gap, these materials are deemed excellent candidates for the window layer in solar cells[1]. Among them, CdS thin films have emerged as highly promising for solar cell applications, boasting 14–16% efficiencies. The wide-band CdS (with an energy gap (E_g) of 2.4 eV) has been successfully employed as a window material in conjunction with various semiconductors such as CdTe [2], Cu_2S [3], InP [1], and $CuInSe_2$[4]. Despite its efficacy, Because CdS is expensive, scientists are concentrating on polycrystalline compound semiconductors, especially polycrystalline films[57]. Various methods have been explored for the

---

* Corresponding author: muhannadjadan99@gmail.com
https://doi.org/10.15251/CL.2025.221.77

preparation of CdS films, including Chemical Bath Deposition (CBD) [8], Molecular Beam Epitaxy (MBE) [9], CSP [10], and sol-gel [11,12]. Among these techniques, CSP is a practical, cost-effective method [13-16]. It has proven capable of producing high-quality semiconductors, enabling the fabrication of solar cells with satisfactory efficiency. This paper aims to fabricate CdS: Al thin films via CSP to analyze their topography, optical properties, and structural characteristics.

2. Experimental

Using the spray pyrolysis method, cadmium chloride $CdCl_2$ (purity: 99.99%) from Sigma-Aldrich obtained thin cadmium sulfide (CdS) films. Aluminum chloride dopant had a volumetric ratio of 2% and 4%. Merck Germany manufactured it. The resulting solutions were deposited on glass substrates using compressed air that was kept at a pressure of 10^5 Nm^{-2} at a flow rate of 4.5 ml/min, deposition time of 8 sec, and a 2 min delay to prevent overcooling. The temperature of the substrate was kept constant at 450 °C. A gap of approximately 29 cm was maintained between the spray nozzle and the heater. The circumstances of this deposit allow for the production of high-quality films. They are consistent in appearance and strongly adhere to the base surface. The film's thickness was determined using the gravimetric method, and the values were 330 ± 25 nm. XRD and AFM were obtained to clarify films structure and morphology. Scanning Electron Microscopy (SEM) was utilized for morphological analysis. Optical transmittance is recorded employing UV-VIS spectrophotometer. Gas sensitivity was evaluated using the percentage change in resistance in a cylindrical chamber (radius: 9.5 cm, height: 19 cm).

3. Results and discussions

The X-ray diffraction (XRD) spectra of grown films are shown in Figure 1. It can be shown that the XRD peaks are situated at 31.73°, 36.96°, 45.70°, and 66.21°, respectively, and that these angles can be attributed to the (011), (101), (021), and (220) planes [17, 18]. ICDD card no. (43-0985) is used to identify the diffraction peaks as CdS. This demonstrates that the particles have a potent (101) reflection plane. No additional peaks may be attributed to crystalline impurities. All of the doped samples exhibited a shift in the position of their diffraction peaks toward higher angles. The shift may result from the smaller ionic radius of Al^{3+} (0.675) compared to that of Cd^{2+} (0.97). The shifting of the XRD peaks is assured that Al dopant has been incorporated into the crystal lattice of the host material, which is CdS.[19, 20]

The grain size (D)of the prepared thin films is obtained using Scherrer's formula, which is shown below. [21, 22]:

$$D = \frac{0.9\lambda}{\beta\cos\theta} \tag{1}$$

where λ X-ray wavel
ength,β (FWHM), and θ Bragg's angle. Undoped CdS, CdS:2% Al, and CdS:4% thin films exhibited D of 13.51 nm, 12.69 nm, and 12.41 nm, respectively, as listed in Table 1. The increase in D is attributed to Aluminum doping-induced grain development [23,24].

The dislocation density (δ) is calculated using the equation [25].

$$\Delta = \frac{1}{D^2} \tag{2}$$

Eq. 3 [26] was utilized to assess the strain (ε).

$$\varepsilon = \frac{\beta\cos\theta}{4} \tag{3}$$

The decrease in dislocation density from 66.52 to 54.78 and the strain parameter's reduction from 28.55 to 25.66, as observed in Table 1, indicate the improved crystalline quality of the thin films with increasing Aluminum doping. Dislocations are structural defects within a crystal lattice that can impact mechanical and electronic properties. Similarly, the decline in the strain parameter signifies lattice strain relaxation within the material. Higher levels of Aluminum doping lead to a more relaxed lattice structure, reducing strain and enhancing thin film stability and performance in practical applications[27, 28]. This trend is further illustrated in Figure (2), which plots FWHM, dislocation density, and strain against various levels of Aluminum doping.

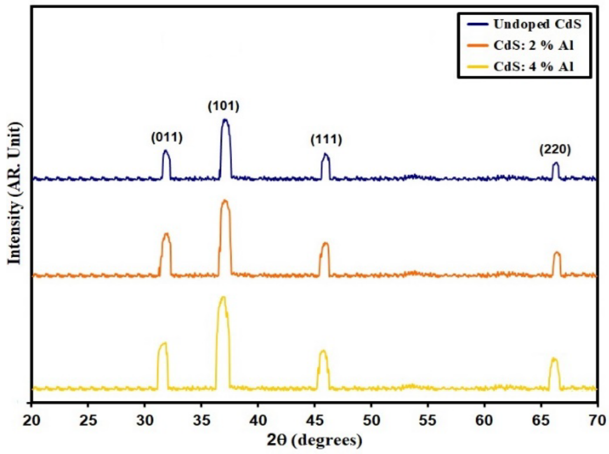

Fig. 1. XRD pattern of Undoped CdS and doping with aluminum films.

Table 1. Structural parameters of Undoped CdS and doping with Ag films.

Samples	2θ(°)	(hkl) Plane	FWHM (°)	E_g (eV)	D (nm)	Dislocations density ($\times 10^{14}$)(lines/m^2)	Strain $\times 10^{-4}$
Undoped CdS	36.96	101	0.69	2.51	12.14	66.50	28.55
CdS : 2% Al	36.93	101	0.66	2.45	12.69	62.09	27.31
CdS : 4% Al	36.89	101	0.62	2.38	13.51	54.78	25.66

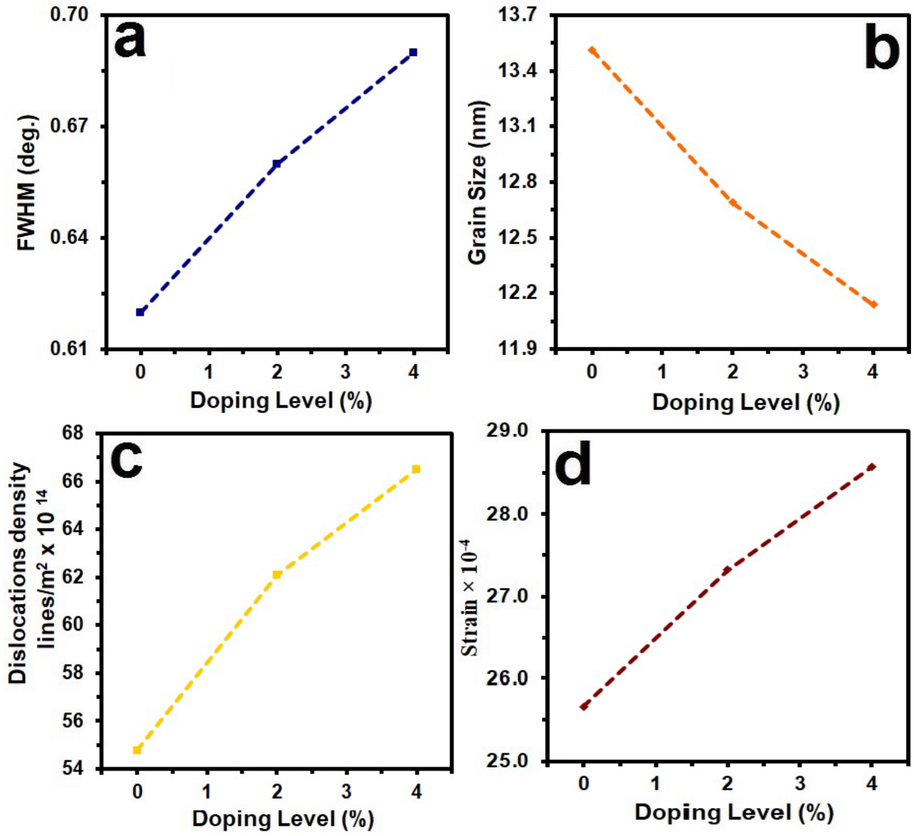

Fig. 2. FWHM, strain and dislocation of undoped and CdS: Al films with different dopant.

Atomic Force Microscope (AFM) was employed to examine the surface topography of the deposited films. Figure 3 presents a 3D AFM image of undoped CdS thin films (a_1, b_2, and c_1), revealing larger grain sizes, indicating highly crystalline films with good surface morphology. Table 1 details the produced films' average roughness (Ra) and root mean square roughness (Rrms). For CdS films deposited with 2% Al and 4% Al, grain sizes are observed at 78.46 nm, 69.75 nm, and 42.20 nm, respectively. The roughness parameters of CdS decrease as Al content rises, RMS value of 12.41 nm to 3.38 nm as a function of Al dopant concentration, as illustrated in Figure 3. Table 2 highlights the impact of Al doping on average particle size, showing an increase in its values due to doping [29, 30].

Table 2. The Morphological values of Undoped and CdS: Al films with different dopants.

Samples	Average Particle size nm	Ra (nm)	RMS (nm)
CdS	78.46	9.74	12.41
CdS : 2% Al	69.75	5.55	9.25
CdS : 4% Al	42.20	5.16	3.38

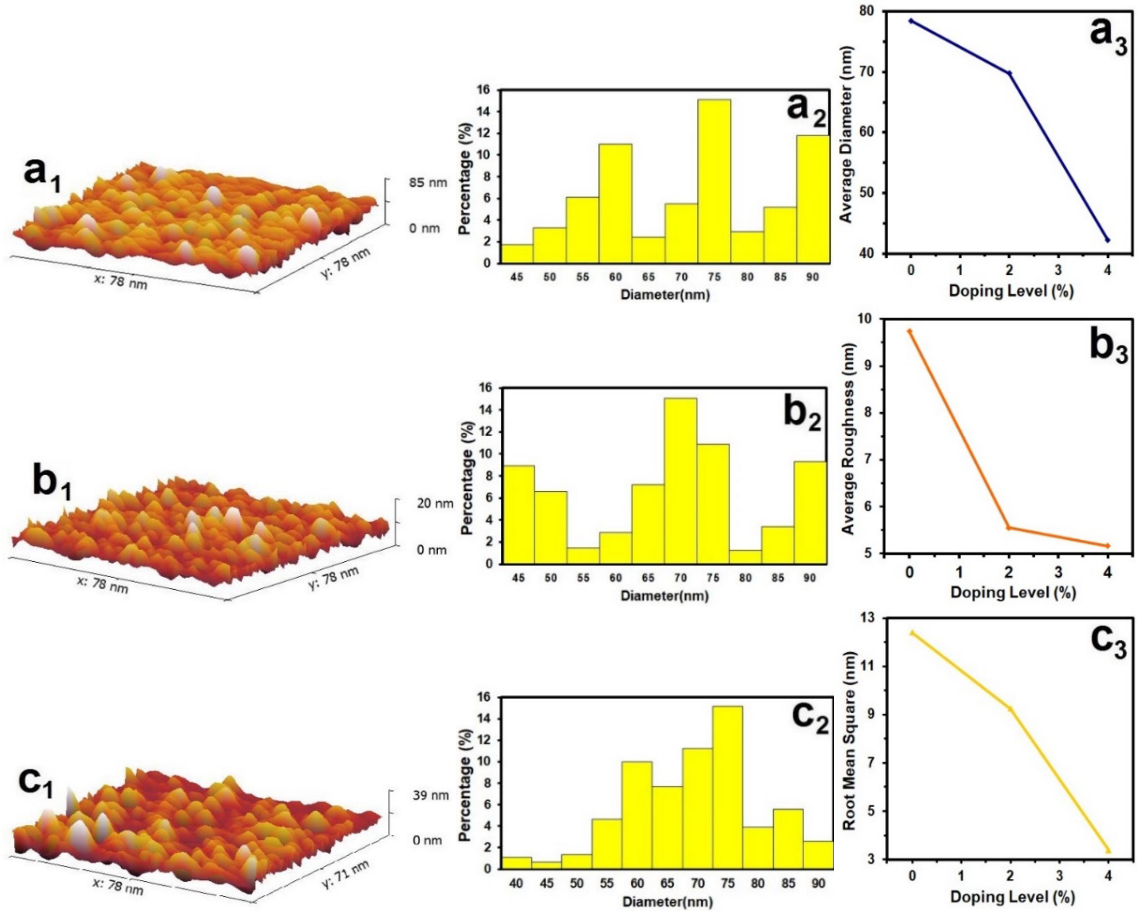

Fig. 3. AFM information.

The SEM images in Fig. (4) showcase the morphological evolution of the synthesized films derived from Undoped CdS, CdS: 2% Al, and CdS: 4% Al. The initial characterization reveals flat islands on the film's surface, representing the Undoped CdS condition. However, a remarkable transformation occurs with the introduction of Aluminum doping, leading to a uniform coverage of spherical nano-grains. The observed decrease in the size of these nano-grains with increasing Al doping levels suggests a direct relationship between Al concentration and the resulting nanostructure. This phenomenon is likely influenced by the intricate interaction between the introduced Aluminum and the CdS matrix, impacting the growth and arrangement of nanostructures during the film synthesis process [31, 32].

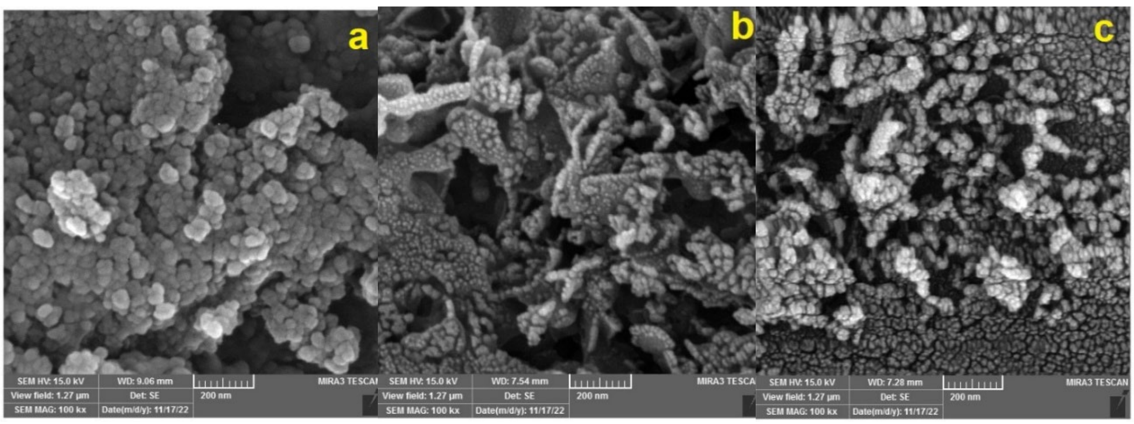

Fig. 4. SEM images of CdS: (a) Undoped, (b) 2% Al, (c) 4% Al.

Experimental measurements are commonly presented using the percentage transmittance (T), defined as [33]:

$$T\% = \frac{I}{I_o}\% \tag{4}$$

where (I) is the light intensity after it passes through the sample and (Io) is the initial light intensity. The prepared films' transmittance is shown in Figure 5 The undoped film exhibits good transparency in the Vis region with values greater than 67%. As the amount of Aluminum in the material rises, the average transmittance falls from 58%. Lattice flaws could be blamed for this drop [34, 35]. Compared to undoped film, the spectra of the Al-doped films demonstrated a lower degree of transparency. The scattering of photons is increased by adding Al, which may result in a decrease in transmittance. This result agrees well with Bairy et al.[36]

It was possible to determine the absorption coefficient (α) by applying the following relation [37]:

$$\alpha = \frac{1}{d} ln \frac{1}{T} \tag{5}$$

where T is the transmittance and d is film thickness in cm. The correlation between and photon energy is shown in Figure 5. Figure (6) shows that the absorption edge increases as the aluminium content increases. This is due to the quantum confinement effect, which is confirmed by the blue shift in the absorption peaks compared to bulk material. The absorbance peak of Al-doped CdS occurs somewhere about 495 nm. Generally, the absorbance is determined by several parameters: oxygen deficiency, E_g, impurity centers, *D*, ε, and R_a [38].

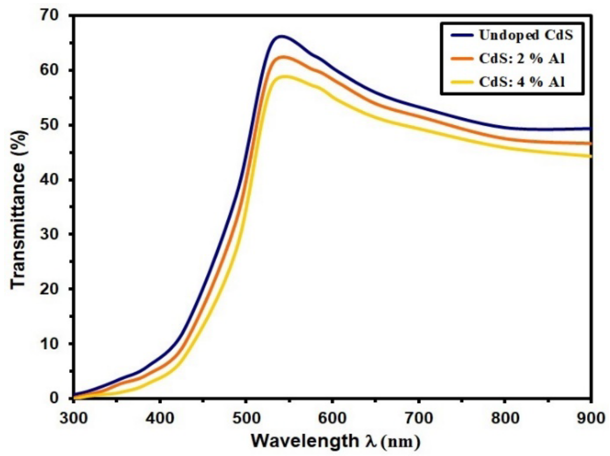

Fig. 5. Transmittance of grown films.

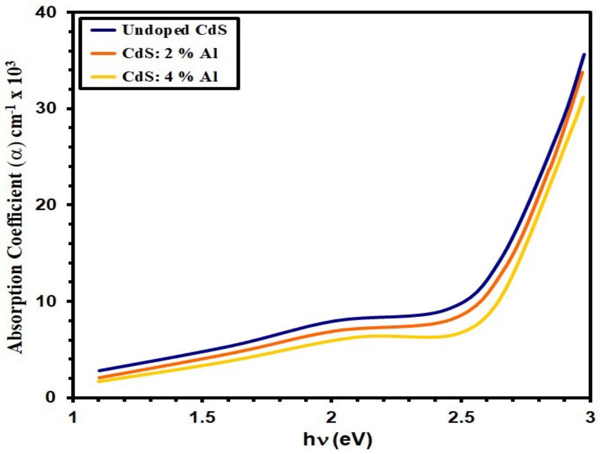

Fig. 6. Absorption coefficient α with wavelength of Undoped and CdS: Al films with different dopants.

The optical band E_g of undoped CdS and CdS: Al films can be determined using Tauc's relation [39] by inter-band absorption theory.

$$(\alpha h\nu) = A\left(h\nu - E_g\right)^{\frac{1}{2}} \tag{6}$$

where hν is the photon energy, and A is a constant. Figure 7 illustrates that the bandgap (Eg) of CdS thin films varies with Al concentration, increasing as the Al content rises. According to Table 1, the bandgap values for CdS, CdS with 2% Al, and CdS with 4% Al thin films were measured at 2.38 eV, 2.45 eV, and 2.51 eV, respectively. This indicates that Al doping influences the bandgap of CdS thin films [40].

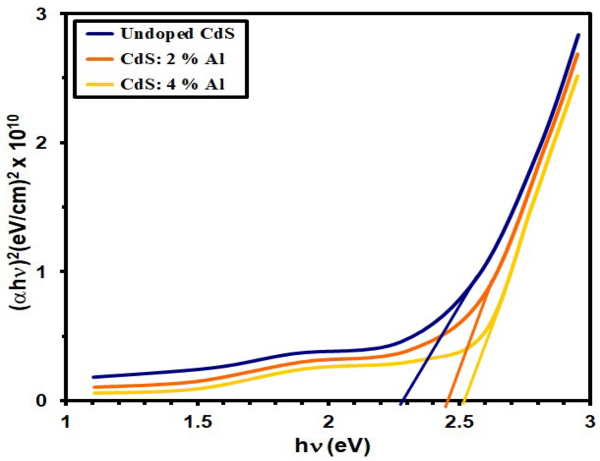

Fig. 7. E_g of Undoped and CdS: Al films with different dopants.

The refractive index (n) and the extinction coefficient (k) of the films at various wavelengths can be obtained employing the relations [41]:

$$n = \frac{1 + R^{\frac{1}{2}}}{1 - R^{\frac{1}{2}}} \tag{7}$$

where R is the optical reflectance [42].

$$K = \frac{\alpha\lambda}{4\pi} \tag{8}$$

Refractive index of the produced films was determined. Figure 8 illustrates the fluctuation of the refractive index with wavelength, showing a consistent pattern for all films. The refractive index values range from 3.14 to 3.07 at long wavelengths, indicating increased film density due to the doping process [43]. A smaller grain size may lead to higher light dispersion within the film, causing light to travel more slowly through the CdS: Al films and increasing the materials' refractive index [44]. Figure 9 illustrates the relationship between the extinction coefficient and wavelength for all films. Despite fluctuations corresponding to the wavelength of polarized light, all films exhibit a consistent trend. After Al doping, there is a slight decrease in the extinction coefficient. This suggests a correlation between the material's extinction coefficient and absorption properties, indicating alterations in its light absorption characteristics following Al doping [45, 46].

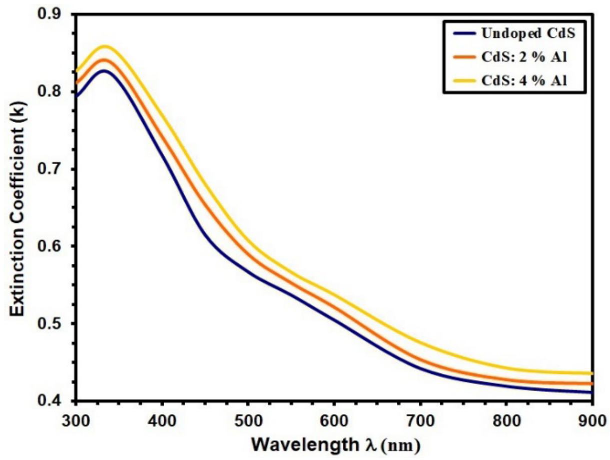

Fig. 8. n of the grown films.

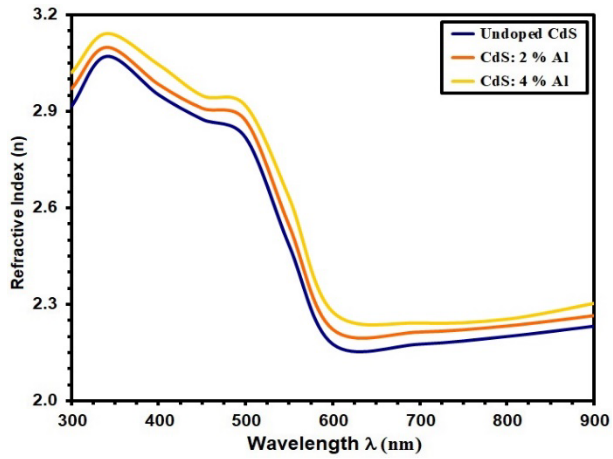

Fig. 9. k of the grown films.

The increase in resistance of the CdS film upon exposure to NO_2 gas at an operational temperature of 125°C indicates its gas-sensing capability towards NO_2 [47]. This rise in resistance reflects the interaction between NO_2 molecules and the CdS film, altering its electrical conductivity. Typically, NO_3 gas reduces the number of free charge carriers in the film, increasing resistance. Additionally, Aluminum doping in the CdS film may affect its gas-sensing properties [48]. Figure (11) likely illustrates gas response curves for undoped CdS and CdS: Al films, offering visual insights into their gas-sensing behavior.

Sensor response can be calculated with equation [49].

$$Sensitivity = \frac{\Delta R}{R_g} = \left|\frac{R_g - R_a}{R_g}\right| \times 100\ \% \tag{9}$$

Figure (12) illustrates the sensitivity of undoped CdS and CdS films doped with 2% and 4% Al to various concentrations of NO_2 gas (75, 150, and 225 ppm). Sensitivity decreases with Aluminum doping, likely due to hindered gas diffusion [50]. CdS: 4% Al films exhibit reduced sensitivity, possibly because Aluminum doping impedes gas diffusion. Decreased sensitivity percentages for different NO_2 concentrations suggest that thinner CdS films improve responsiveness to NO_2 gas [51].

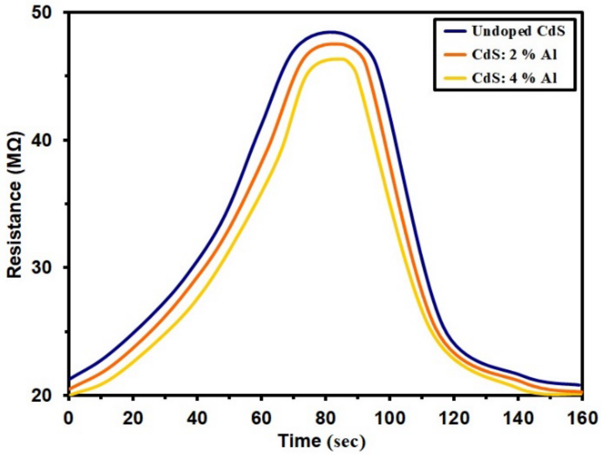

Fig. 11. illustrates resistance over time for undoped CdS and CdS: Al films with various dopant concentrations.

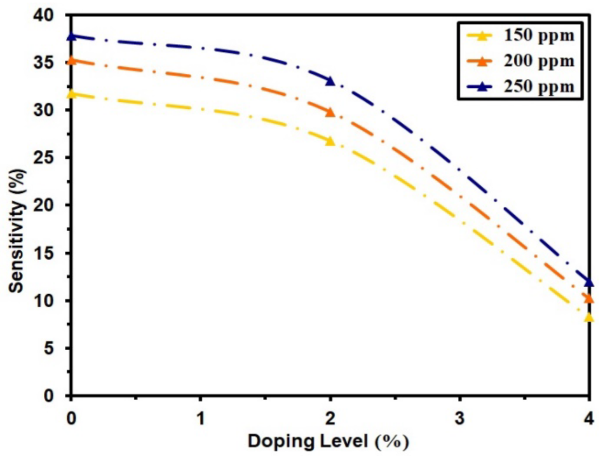

Fig. 12. Displays the sensitivity of undoped CdS and CdS: Al films with varying dopant concentrations.

4. Conclusion

A thin film of CdS films was deposited via Al concentrations. The XRD results showed that the CdS film was polycrystalline with a predominant plane (101). With CdS:4% Al, the grain size of the undoped CdS molecule is approximately (12.51–12.14 nm), and the strain has decreased from

28.55 to 25.66. A study of surface morphology reveals that higher concentrations of aluminium-doped CdS thin films were of high quality. The AFM analysis showed that the nanostructured of CdS, CdS:2% Al, and CdS:4% Al, had smooth surfaces with smaller particle sizes:78.46, 69.75, and 42.20 nm as Al content rise. SEM images show CdS film evolution: flat islands (Undoped CdS) transform to uniform spherical nano-grains with Al doping. Separately, evidence on thin films in the UV-VIS spectrum showed that the aluminium content will affect the optical properties of CdS thin films. The optical band gap, e.g., rises with increasing Al doping from (2.38 to 2.51) eV. The extinction coefficient and refractive index decreased with the Aluminum. CdS film detects NO_2, altering resistance. Aluminium doping may influence sensing. The sensitivity of CdS to NO_2 decreases with Al doping. Thinner films enhance responsiveness.

Acknowledgements

Mustansiriyah University and Alnukhba University College provided financial support for this project, for which the authors are grateful.

References

[1] J. Han, C. Spanheimer, G. Haindl, G. Fu, V. Krishnakumar, J. Schaffner, C. Fan, K. Zhao, A. Klein, W. Jaegermann, Sol. Energy Mater. Sol. C, 95 (3), 816-820, (2011); https://doi.org/10.1016/j.solmat.2010.10.027
[2] R. Mariappan, V. Ponnuswamy, M. Ragavendar, D. Krishnamoorthi, C. Sankar, Optik, 123, 1098-1102 (2012); https://doi.org/10.1016/j.ijleo.2011.07.038
[3] D. A. Mazón-Montijoa, M. Sotelo-Lerma, L. Rodríguez-Fernández, L. Huerta, Applied Surface Science, 256, 4280-4287, (2010); https://doi.org/10.1016/j.apsusc.2010.02.015
[4] M. Contreras, M. Romero, B. To, F. Hasoon, R. Noufi, S. Ward and K. Ramanathan, Thin Solid Films, 403-404 (579), 204-211 (2002); https://doi.org/10.1016/S0040-6090(01)01538-3
[5] A. Davis, K. Vaccaro, H. Dauplaise, W. Waters and J. Lorenzo, Journal of the Electrochemical Society, 146 (3), 1046-1053 (1999); https://doi.org/10.1149/1.1391719
[6] M. Ilieva, D. Dimova-Malinovska, B. Ranguelov and I. Markov, Journal of Physics: Condensed Matter, 11 (49), 10025-10031 (1999);. https://doi.org/10.1088/0953-8984/11/49/320
[7] F. A. Jasima , Z. S. A. Mosa, N. F. Habubi, Y. H. Kadhim, S. S. Chiad, Digest Journal of Nanomaterials and Biostructures, 18 (3), 1039–1049 (2023); https://doi.org/10.15251/DJNB.2023.183.1039
[8] O. Vigil-Galan, J. Ximel-lo-Quiebras, J. Aguilar-Hernandez, G. Contreras-Puente, A. Cruz-Orea, J. Mendoza-Alvarez, J. Cardona-Bedoya, C. Ruiz and V. Bermudez, Semiconductor Science and Technology, 21, 76 (2006); https://doi.org/10.1088/0268-1242/21/1/014
[9] P. Boieriu, R. Sporken, Y. Xin, N. Browning and S. Sivananthan, Journal of Electronic Materials, 29 (6), 718-722 (2000); https://doi.org/10.1007/s11664-000-0212-3
[10] Salih Yılmaz, The investigation of spray pyrolysis grown CdS thin films doped with fluorine atoms. Applied Surface Science 357, 873–879, (2015); https://doi.org/10.1016/j.apsusc.2015.09.098
[11] M.S. Sivakumar, Structural, Journal of Materials Science: Materials in Electronics, 28 (17), 12432-12439, (2017); https://doi.org/10.1080/02670844.2017.13039
[12] A. Kerimova, E. Bagiyev, E . Aliyeva, et al., Phys. Status Solidi C, 14 (6), 1600144 (2017); https://doi.org/10.1002/pssc.201600144
[13] D. Herrera-Molina , J.E. Diosa , A. Fern´andez-P´erez , E. Mosquera-Vargas, Materials Science and Engineering B 273, 115451 (2021); https://doi.org/10.1016/j.mseb.2021.115451
[14] E. Pino, C. Calderón, F. Herrera, G. Cifuentes, G. Arteaga, Front. Chem. 8, 1 (2020); https://doi.org/10.3389/fchem.2020.00365
[15] T. K. Ghorai, N. Biswas, J. Mater. Res. Technol. 2, 10 (2013).
[16] F. Soleimani, A. Nezamzadeh-Ejhieh, J. Mater. Res. Technol. 9, 16237 (2020);

https://doi.org/10.1016/j.jmrt.2020.11.091
[17] A. S. Al Rawas, M. Y. Slewa, B. A. Bader, N. F. Habubi, S. S. Chiad, Journal of Green Engineering,10 (9), 7141-7153 (2020); https://doi.org/10.1021/acsami.1c00304
[18] R. S. Ali, H. S. Rasheed, N. F. Habubi, S.S. Chiad, Chalcogenide Letters,, 20 (1), 63–72 (2023; https://doi.org/10.15251/CL.2023.201.63
[19] N. Y. Ahmed, B. A. Bader, M. Y. Slewa, N. F. Habubi, S. S. Chiad, NeuroQuantology, 18(6), 55-60 (2020); https://doi.org/10.1016/j.jlumin.2021.118221
[20] R. S. Ali, M. K. Mohammed, A. A. Khadayeir, Z. M. Abood, N. F. Habubi and S. S. Chiad, Journal of Physics: Conference Series, 1664 (1), 012016 (2020); https://doi:10.1088/1742-6596/1664/1/012016
[21] A. A. Khadayeir, R. I. Jasim, S. H. Jumaah, N. F, Habubi, S. S. Chiad, Journal of Physics: Conference Series,1664 (1) (2020); https://doi.org/10.1088/1742-6596/1664/1/012009
[22] O. M. Abdulmunem, A. M. Jabbar, S. K. Muhammad, M. O. Dawood, S. S. Chiad, N. F. Habubi, Journal of Physics: Conference Series,1660 (1), 012055 (2020); https://doi.org/ 10.1088/1742-6596/1660/1/012055
[23] A. A. Khadayeir, K. H. Abass, S. S. Chiad, M. K. Mohammed, N. F. Habubi, T. K. Hameed, I. A. Al-Baidhany, Journal of Engineering and Applied Sciences, 13 (22), 9689-9692 (2018).
[24] A. Ghazai, K. Qader, N. F. Habubi, S. S. Chiad, O. Abdulmunem, IOP Conference Series: Materials Science and Engineering, 870 (1), 012027 (2020); https://doi.org/ 10.1088/1757-899X/870/1/012027
[25] M. Ilieva, D. Dimova-Malinovska, B. Ranguelov and I. Markov, Journal of Physics: Condensed Matter, 11(49), 10025-10031 (1999); https://doi.org/10.1088/0953-8984/11/49/320
[26] B. A. Bader, S. K. Muhammad, A. M. Jabbar, K. H. Abass, S. S. Chiad, N. F. Habubi, J. Nanostruct, 10 (4): 744-750, (2020); https://doi.org/ 10.22052/JNS.2020.04.007
[27] F. H. Jasim, H. R. Shakir, S. S. Chiad,N. F. Habubi, Y. H. Kadhi,, Jadan, M., Digest Journal of Nanomaterials and Biostructures, 18(4), 1385–1393 (2023); https://doi.org/10.15251/DJNB.2023.184.1385
[28] E. H. Hadi, M. A. Abbsa, A. A. Khadayeir, Z. M. Abood, N. F. Habubi, S. S. Chiad, Journal of Physics: Conference Series, 1664 (1), 012069 (2020); https://doi.org/ 10.1088/1742-6596/1664/1/012069
[29] H. T. Salloom, R. I. Jasim, N. F. Habubi, S. S. Chiad, M. Jadan, J. S. Addasi, Chinese Physics B, 30 (6), 068505 (2021); https://doi.org/10.1088/1674-1056/abd2a7
[30] S. S Chiad,, A. S. Alkelaby, K. S. Sharba,, Journal of Global Pharma Technology, 11 (7), 662-665, (2020); https://doi.org/10.1021/acscatal.1c01666
[31] S. S. Chiad, H. A. Noor, O. M. Abdulmunem, N. F. Habubi, Journal of Physics: Conference Series, 1362 (1), 012115 (2019); https://doi.org/10.1088/1742-6596/1362/1/012115
[32] C. K. Sheng, Y. M. Alrababah, Kuwait J. Sci. 49, 1 (2022); https://doi.org/10.48129/kjs.11913
[33] R. I. Jasim, E. H. Hadi, S. S. Chiad, N. F. Habubi, M. Jadan, J. S. Addasi, Journal of Ovonic Research, 19 (2), 187 – 196 (2023); https://doi.org/10.15251/JOR.2023.192.187
[34] E. H. Hadi, D. A. Sabur, S. S. Chiad, N. F. Habubi, K., Abass, Journal of Green Engineering, 10 (10), 8390-8400 (2020); https://doi.org/10.1063/5.0095169
[35] E. S. Hassan, K. Y. Qader, E. H. Hadi, S. S. Chiad, N. F. Habubi, K. H. Abass, Nano Biomedicine and Engineering, 12(3), pp. 205-213 (2020); https://doi.org/10.5101/nbe.v12i3.p205-213
[36] M. D. Sakhil, Z. M. Shaban, K. S. Sharba, N. F. Habubi, K. H. Abass, S. S. Chiad, A. S. Alkelaby, NeuroQuantology, 18 (5), 56-61 (2020); https://doi.org/10.14704/nq.2020.18.5.NQ20168
[37] M. S. Othman, K. A. Mishjil, H. G. Rashid, S. S. Chiad, N. F. Habubi, I. A. Al-Baidhany, Journal of Materials Science: Materials in Electronics, 31(11), 9037-9043 (2020); https://doi.org/10.1007/s10854-020-03437-0
[38] K. Y. Qader, R. A. Ghazi, A. M. Jabbar, K. H. Abass, S. S. Chiad, Journal of Green Engineering, 10 (10), 7387-7398 (2020); https://doi.org/10.1016/j.jece.2020.104011

[39] K. S. Sharba, A. S. Alkelaby, M. D. Sakhil, K. H. Abass, N. F. Habubi, S. S. Chiad, Enhancement of urbach energy and dispersion parameters of polyvinyl alcohol with Kaolin additive, NeuroQuantology, 18 (3), 66-73 (2020); https://doi.org/10.14704/NQ.2020.18.3.NQ20152
[40] A. A. Khadayeir, E. S. Hassan, S. S. Chiad, N. F. Habubi, K. H. Abass, M. H. Rahid, T. H. Mubarak, M. O. Dawod, I. A. Al-Baidhany, Journal of Physics: Conference Series 1234 (1), 012014, (2019); https://doi.10.88/1742-6596/1234/1/012014
[41] A. S. Alkelaby, K. H. Abass, T. H. Mubarak, N. F. Habubi, S. S. Chiad, I. Al-Baidhany, Journal of Global Pharma Technology 11(4), 347-352 (2019).
[42] K. Y. Qader, E. H. Hadi, N. F. Habubi, S. S. Chiad, M. Jadan, J. S. Addasi, International Journal of Thin Films Science and Technology, 10 (1), 41-44 (2021); https://doi.org/ 10.18576/ijtfst/100107
[43] N. N. Jandow, M. S. Othman, N. F.Habubi, S. S. Chiad, K. A. Mishjil, I. A. Al-Baidhany, Materials Research Express, 6 (11), (2020); https://doi.org/10.1088/2053-1591/ab4af8
[44] M. O. Dawood, S. S. Chiad, A. J. Ghazai, N. F. Habubi, O. M. Abdulmunem, AIP Conference Proceedings 2213, 020102,(2020); https://doi.org/10.1063/5.0000136
[45] S. S. Chiad, K. H. Abass, T. H. Mubarak, N. F. Habubi, M. K. Mohammed, A. A. , Khadayeir, Journal of Global Pharma Technolog, 11(4), 369-375 (2019).
[46] E. S. Hassan, T. H. Mubarak, S. S. Chiad, F. N. Habubi, A. A. Khadayeir, M. O. Dawood, I. A. Al-Baidhany, Journal of Physics: Conference Series, 1294(2), 022008 (2019); https://doi.10.88/1742-6596/1294/2/022008
[47] S. K. Muhammad, M. O. Dawood, N. Y. Ahmed, E. S. Hassan, N. F. Habubi, S. S. Chiad, Journal of Physics: Conference Series, 1660 (1), 012057 (2020); https://doi.org/ 10.1088/1742-6596/1660/1/012057
[48] B. A. Bader, S. K. Muhammad, A. M. Jabbar, K. H. Abass, S. S. Chiad, N. F. Habubi, J. Nanostruct, 10 (4): 744-750, (2020).
[49] O. M. Abdulmunem, A. M. Jabbar, S. K. Muhammad, M. O. Dawood, S. S. Chiad, N. F. Habubi, Journal of Physics: Conference Series,1660 (1), 012055 (2020); https://doi.org/10.1088/1742-6596/1660/1/012055
[50] A.K. Vishwakarma, S.S. Majid, L. Yadava, Vacuum, 165, 239–245 (2019); https://doi.org/10.1016/j.vacuum.2019.04.040
[51] E. H. Hadi, M. A. Abbsa, A. A. Khadayeir, Z. M. Abood, N. F. Habubi, S.S. Chiad, Journal of Physics: Conference Series, 1664 (1), 012069 (2020); https://doi.org/10.1088/1742-6596/1664/1/012069
[52] R. S Ali, N. A. H. Al Aaraji, E. H. Hadi, N. F. Habubi, S. S. Chiad, Journal of Nanostructuresthis link is disabled, 10(4), 810–816 (2020); https://doi: 10.22052/jns.2020.04.014
[53] S. K. Muhammad, N. D. M. Taqi, S. S. Chiad, K. H. Abass, N. F. Habubi, Journal of Green Engineering, 11(2), 1287-1299 (2021).
[54] A. A. Abdul Razaq, F. H. Jasim, S. S. Chiad F. A. Jasim, Z. S. A. Mosa , Y. H. Kadhimd, Journal of Ovonic Research, 20 (2), 131 – 141 (2024); https://doi.org/10.15251/JOR.2024.202.131
[55] E. S. Hassan, D. M. Khudhair, S. K. Muhammad, A. M. Jabbar, M.O. Dawood, N. F. Habubi, S. S. Chiad, Journal of Physics: Conference Series ,1660 (1) 1660 012066 (2020); https://doi.org/10.1088/1742-6596/1660/1/012066
[56] A. J. Ghazai, O. M. Abdulmunem, K. Y. Qader, S. S. Chiad, N. F. Habubi, AIP Conference Proceedings 2213 (1), 020101 (2020); https://doi.org/10.1063/5.0000158
[57] H. A. Hussin, R. S. Al-Hasnawy, R. I. Jasim, N. F. Habubi, S. S. Chiad, Journal of Green Engineering, 10(9), 7018-7028 (2020); https://doi.org/10.1088/1742-6596/1999/1/012063
[58] S. S. Chiad, H. A. Noor, O. M. Abdulmunem, N. F. Habubi, M. Jadan, J. S. Addasi, Journal of Ovonic Research, 16 (1), 35-40 (2020). https://doi.org/10.15251/JOR.2020.161.35
[59] H. T. Salloom, E. H. Hadi, N. F. Habubi, S. S. Chiad, M. Jadan, J. S. Addasi, Digest Journal of Nanomaterials and Biostructures, 15 (4), 189-1195 (2020); https://doi.org/10.15251/DJNB.2020.154.1189

[60] A. A. Khadayeir, E. S. Hassan, T. H. Mubarak, S. S. Chiad, N. F. Habubi, M. O. Dawood, I. A. Al-Baidhany, Journal of Physics: Conference Series, 1294 (2) 022009(2019); https://doi.1088/1742-6596/1294/2/022009
[61] A. Davis, K. Vaccaro, H. Dauplaise, W. Waters and J. Lorenzo, Journal of the Electrochemical Society, 146 (3), 1046-1053 (1999); https://doi.org/10.1016/j.matlet.2017.05.117
[62] M. Ilieva, D. Dimova-Malinovska, B. Ranguelov and I. Markov, Journal of Physics: Condensed Matter, 11(49), 10025-10031 (1999); https://doi.org/10.1088/0953-8984/11/49/320